### Title

Teeth, prenatal growth rates, and the evolution of human-like pregnancy in later Homo




### Journal

Proceedings of the National Academy of Sciences of the United States of America, 119(41)

### ISSN

0027-8424



### Authors

Monson, Tesla A
Weitz, Andrew P
Brasil, Marianne F
et al.



### Publication Date

2022-10-11

### DOI

10.1073/pnas.2200689119

Peer reviewed

PNAS RESEARCH ARTICLE | ANTHROPOLOGY OPEN ACCESS

# Teeth, prenatal growth rates, and the evolution of human-like pregnancy in later *Homo*

Tesla A. Monson[a,1], Andrew P. Weitz[b], Marianne F. Brasil[c,d], and Leslea J. Hlusko[d,e,f]

Edited by Peter Ungar, University of Arkansas Fayetteville, Fayetteville, AR; received January 13, 2022; accepted August 26, 2022 by Editorial Board Member C. O. Lovejoy

**Evidence of how gestational parameters evolved is essential to understanding this fundamental stage of human life. Until now, these data seemed elusive given the skeletal bias of the fossil record. We demonstrate that dentition provides a window into the life of neonates. Teeth begin to form in utero and are intimately associated with gestational development. We measured the molar dentition for 608 catarrhine primates and collected data on prenatal growth rate (PGR) and endocranial volume (ECV) for 19 primate genera from the literature. We found that PGR and ECV are highly correlated ($R^2 = 0.93$, $P < 0.001$). Additionally, we demonstrated that molar proportions are significantly correlated with PGR ($P = 0.004$) and log-transformed ECV ($P = 0.001$). From these correlations, we developed two methods for reconstructing PGR in the fossil record, one using ECV and one using molar proportions. Dental proportions reconstruct hominid ECV ($R^2 = 0.81$, $P < 0.001$), a result that can be extrapolated to PGR. As teeth dominate fossil assemblages, our findings greatly expand our ability to investigate life history in the fossil record. Fossil ECVs and dental measurements from 13 hominid species both support significantly increasing PGR throughout the terminal Miocene and Plio-Pleistocene, reflecting known evolutionary changes. Together with pelvic and endocranial morphology, reconstructed PGRs indicate the need for increasing maternal energetics during pregnancy over the last 6 million years, reaching a human-like PGR (i.e., more similar to humans than to other extant apes) and ECV in later *Homo* less than 1 million years ago.**

maternal energetics | dentition | hominid fossil record | prenatal growth | endocranial volume

## Significance

Humans are characterized by having very large brains relative to body size. Because gestation is critically linked to brain size, pregnancy is an important but elusive aspect of hominid evolution. We developed two methods for reconstructing prenatal growth during this earliest phase of life history using brain size and dental morphology. Our results indicate a significant increase in prenatal growth rates (PGRs) throughout the terminal Miocene and Plio-Pleistocene with the evolution of human-like PGRs in later *Homo*, less than 1 million years ago. These results align with fossilized pelvic and cranial anatomy to support the evolution of human-like pregnancy in the Pleistocene and open up possibilities for novel ways to explore the evolution of hominid gestation via dental variation.

Life history describes the schedule and process of growth and development, otherwise known as ontogeny (1, 2). Key milestones in mammalian life history begin early in development with conception and gestation, and proceed throughout the lifespan, ending in death. The earliest stages of primate life history are intricately balanced through the maternal–infant relationship (3). Developing human embryos, like those of other primates, are entirely reliant on their gestating parent throughout prenatal development; it is the only stage of primate life history where a gestating female cannot pass on or distribute any of the metabolic or physiological burden of growing and raising offspring to other members of the social group (3–5). However, a gestating parent can receive support through the community, including through a partner, whether or not they have contributed genetic material to the offspring. This support is almost always linked to resource provisioning and protection from predators (6–8).

The growing body of research on primate maternal energetics, infant growth and development, and the evolution of cognition revolves around a complex network of resource provisioning, maternal health, trophic status, locomotion, body size, infant dependency (sometimes referred to as altriciality), and social network (5, 9–17). The importance of each of these factors in the evolution of the human species is still very much under debate, largely complicated by the difficulty of assessing many of these physiological and behavioral traits in the fossil record. While a large body of research has focused on postnatal growth rates and duration in humans and other hominids (18–20), almost no research has investigated prenatal growth rates (PGRs) in the fossil record. This imbalance is due in part to the prior inability to infer such a complex life history trait from skeletal remains.

Prenatal growth, the rate of embryonic and fetal growth in utero, plays a key role in establishing the trajectory of an individual's metabolism, neurological development, and ultimate growth during their lifetime (21). Calculated as the ratio of birth weight (mass in grams) to gestation length (days) (22), mammalian species that have high rates of prenatal growth have infants that are larger at birth relative to other species with comparable lengths of gestation. In primates, gestational length is relatively similar

Author contributions: T.A.M. designed research; T.A.M. and A.P.W. performed research and analyzed data; T.A.M., A.P.W., M.F.B., and L.J.H. interpreted results; T.A.M. wrote the paper; and A.P.W., M.F.B., and L.J.H. edited the paper.

The authors declare no competing interest.



This article is a PNAS Invited Submission. P.U. is a guest editor invited by the Editorial Board.

[1]To whom correspondence may be addressed. Email: tesla.monson@wwu.edu.

This article contains supporting information online at http://www.pnas.org/lookup/suppl/doi:10.1073/pnas.2200689119/-/DCSupplemental.

Published October 3, 2022.

across the phylogeny, while PGR can vary quite significantly (23, 24), suggesting that growth rate provides a key source of variation upon which primate evolution occurs.

Despite the oft-repeated statement that human infants are secondarily altricial, meaning that they have most of their growing to do after they are born, humans have the highest PGR among primates (25–27). This life history distinguishes humans from even their closest living relatives (26, 28, 29). This high PGR results in human infants that are quite large at birth relative to their time of gestation, with both large neonatal body mass and brain mass compared to other primates (25, 30). Yet, despite this large body and brain mass, at birth the human infant brain is still only 30% of the size of the adult brain, a developmental characteristic that leads to a helpless infant that is highly reliant on parents and other social group members for survival (19, 31).

Cooperative breeding, pair bonding, and group care have been hypothesized as critical factors in the evolution of the human brain and the helpless infant (11, 17, 21, 32–37). The helpless infant requires constant care and attention, which is provided only by the birthing parent unless they can receive some assistance. Research in nonhuman primates shows that mothers who receive assistance are better able to secure resources for themselves and their infants (30, 36, 38). As the brain is a metabolically expensive organ, resource intake is essential for infant brain growth and development (32, 39, 40). This is also true at earlier life history stages, when the fetus is developing in utero (5, 15, 28). Research in cetaceans has demonstrated that brain size in these large and highly social animals is related to PGR as well as gestational length, with growth rate dependent on maternal energetics, including metabolism, resource intake, and other physiological traits involved in gestation (41). This supports the hypothesis that PGRs are also significantly associated with adult endocranial volume (ECV) in primates, which would not be a surprising result since adult ECV is strongly correlated with neonatal ECV in primates (4). Across eutherians, large neonatal and adult relative brain size do not appear to be related to periods of accelerated brain growth during fetal development, as higher encephalization seems to be a product of slower body growth rather than an increased rate of brain growth (42). However, to our knowledge the direct correlation between PGR and adult ECV has not been previously quantified in primates, and so we test this hypothesis here.

Like the brain, teeth begin to form in utero and are thus intimately associated with the developmental processes in mammalian early life history (43, 44). After birth, teeth remain linked to crucial life history landmarks, including weaning, menarche, and sexual activity through mate competition, and have thus been used extensively to reconstruct primate life histories in the fossil record (1, 29, 45–55). Considerable pleiotropy underlies dental development, with genetic and phenotypic variation in individual tooth morphology being shared with body size, craniofacial structures, and other teeth across the dental arch (43, 44, 56, 57). More recent work has demonstrated that these pleiotropic effects extend even to traits in other parts of the body, including those associated with the maternal–infant relationship, such as a lactation (58).

Our previous work in callitrichids linked slow PGRs to third molar loss, providing one of the first lines of evidence that dental morphology may be directly associated with PGR in primates (59). This insight has direct bearing on humans, as third molar reduction remains one of the most distinct dental features of humans compared to other primates (60–62). A large body of work has generated hypotheses for the drivers of third molar reduction and loss in humans, which range from craniofacial reduction, to brain size increases, to changes in diet and technology, and may in fact be related to all of these morphological and behavioral evolutionary shifts; these relationships have yet to be resolved (60, 63, 64). Based on our previous work, we hypothesized that PGR has a direct quantitative relationship with both ECV and third molar reduction in humans. One of the clearest ways to investigate third molar reduction is through quantification of molar proportions (60–63).

In order to test our hypothesis, we collected dental data on extant and fossil primates and calculated the molar module component (MMC), a genetically patterned trait that captures the ratio of the third to first molar length and thus third molar relative size. MMC has been genetically and phenotypically assessed in a range of catarrhine primates (57, 65), including fossil hominids (66, 67), as well as more broadly across mammals (68, 69). All of these studies demonstrate that MMC carries a strong phylogenetic signal and is not driven by dietary adaptation or body size. Given that disruptions to intrauterine growth in humans result in reduced cranial and tooth size (43, 70), the genetic mechanism underlying variation in MMC may be shared between these traits. We present here an investigation of the relationship between MMC and PGR in extant and fossil primates. Our work aims to develop methods for estimating the evolution of PGR in the hominid fossil record and thereby open a window into the evolutionary history of human gestation.

One of the great challenges to human evolutionary research lies in the limitations of the fossil record. Although fossils are an essential resource that provide the only direct line into the past, the factors at play in fossilization result in a vertebrate record that is comprised almost exclusively of fossilized teeth and bones (71). Thus, in order to elucidate the evolution of human life history, researchers are tasked with the critical job of developing new methods for deducing life history details from hard tissues. Reconstructing life history in the fossil record remains a primary focus of human evolutionary studies (49, 72–74), and a large body of research has focused on the evolutionary interplay between brain size and craniodental and pelvic morphology in fossil hominids (75, 76). Considering that PGR is linked to maternal investment and ECV, a clearer understanding of PGRs in fossil hominids is invaluable to the study of the evolution of human gestation and brain size, crucial elements in life history theory. Using extant and fossil primate data, including dental metrics, PGR, and ECV, we tested the following hypotheses:

H1) PGR is highly correlated with ECV in extant catarrhine primates.
H2) Third molar proportions (as captured by MMC) are significantly associated with PGR and ECV in extant catarrhine primates.
H3) Third molar proportions (as captured by MMC) can accurately predict ECV, and thus PGR, in the hominid fossil record.

By testing these hypotheses, we aimed to address two larger outstanding questions about the evolution of life history in humans:

Q1) Have hominoid PGRs increased significantly throughout the Miocene and Plio-Pleistocene?
Q2) When did human-like (i.e., more similar to humans than to other extant apes) PGRs first evolve?

In order to test our hypotheses and answer these essential questions about life history, we developed two models for

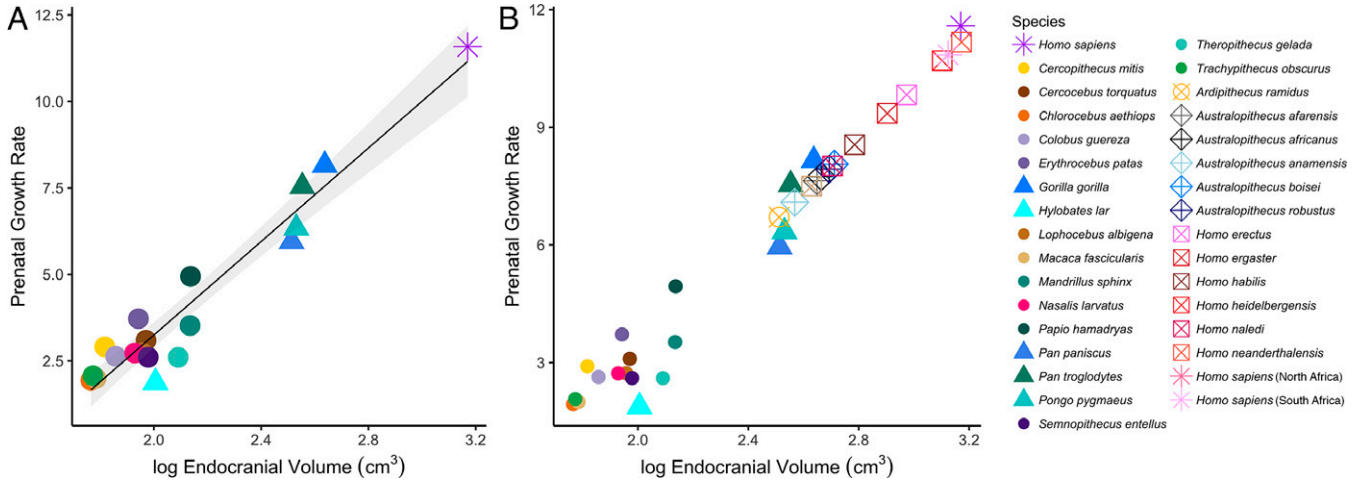


**Fig. 1.** (*A*) PGR (g/day) is significantly correlated with log-transformed ECV in extant catarrhines ($R^2$ = 0.93, $P$ < 0.001). (*B*) PGRs of fossil hominids, reconstructed from fossil ECV measurements, are plotted alongside extant catarrhines. Values were reconstructed via a linear regression model developed from extant data (Table 1). *Homo sapiens* are labeled with an asterisk, extant cercopithecids are labeled with a circle, extant nonhuman apes are labeled with a triangle, *Ardipithecus* is marked with a crossed circle, *Australopithecus* are marked with a crossed diamond, and nonhuman fossil *Homo* species are marked with a crossed square. *Homo sapiens* (North Africa) and (South Africa) are fossil samples. See *SI Appendix*, Figs. S3 and S4 for mandibular MMC results. See *SI Appendix* text for notes on morphospace clustering.

predicting PGR (infant body mass in grams divided by gestation length in days) in the fossil record by using statistical relationships between PGR, ECV, and molar proportions (third molar length relative to first molar length, MMC) in extant catarrhines ($n$ = 608). We present evidence that fossil PGRs can be predicted from both ECV and MMC and thus provide two methods for investigating life history in the fossil record. The relationship between ECV and PGR is extremely tight, while the dental model has more variable predictions, probably due to the impacts of derived craniofacial morphology (e.g., extreme prognathism). To check that dental proportions accurately reconstruct PGR and ECV, we validated our dental model through a quantitative comparison of predicted and observed ECV in the hominid fossil record ($n$ = 13 species). Additionally, we statistically compared the results from both models and assessed the evolution of PGR over the last 6 million years of the hominid fossil record.

## Results

We demonstrated that measurements from both fossil crania and fossil postcanine dentitions can be used to reconstruct PGR in the fossil record. Both of our methods provided consistent and statistically significant results: PGRs have increased over the last 6 million years in hominids, and a human-like PGR evolved less than 1 million years ago in later *Homo*. We define *human-like* as more similar to humans than to other extant apes. Gorillas have the highest PGR of all nonhuman apes at 8.16 g/day, while humans have a PGR of 11.58 g/day, making a PGR of 9.87 g/day the midpoint between humans and the other great apes. Thus, we classify any PGR greater than 9.87 g/day as human-like, rather than nonhuman ape-like.

**ECV Predicts Increasing Prenatal Growth Rates in the Hominid Fossil Record.** ECV is highly and significantly correlated with PGR in extant catarrhines ($R^2$ = 0.93, $P$ < 0.001; Fig. 1*A* and Table 1). Thus, ECV is a strong indicator of PGR and, in turn, maternal physiological investment during gestation. From this statistical relationship observed in extant taxa, we developed a model to predict PGR from ECV. Using ECV measured from fossil crania, we were then able to predict PGR in 13 fossil hominid species (Fig. 1*B* and Table 2). Our model indicates that early hominids (*Ardipithecus* and *Australopithecus*) had PGRs similar to extant nonhuman apes. PGR is predicted to have exceeded rates seen in extant nonhuman apes in *Homo habilis* and *Homo ergaster*, ~1.5–2 million years ago. *Homo erectus* is predicted to have had a relatively high PGR (9.83 g/day, Table 2), and later *Homo* (*H. heidelbergensis*, *H. neanderthalensis*, and fossil *H. sapiens*) are all predicted to have had a human-like PGR (PGR > 9.87 g/day). It is not until fossil *H. sapiens* and *H. neanderthalensis* that we predict a PGR that is the same as

**Table 1. Linear regression models and statistical significance**

| Linear regression model | Equation | $R^2$ | $F$ ($df$) | $P$ |
|---|---|---|---|---|
| PGR ~ Maxillary MMC | $y = -214.70x + 97.18x^2 + 121.01$ | 0.50 | 7.98 (2, 16) | 0.0039 |
| Log-transformed ECV ($cm^3$) ~ Maxillary MMC | $y = -34.86x + 15.90x^2 + 20.98$ | 0.57 | 10.75 (2, 16) | 0.0011 |
| PGR ~ Log-transformed ECV ($cm^3$) | $y = 6.76x - 10.27$ | 0.93 | 233.20 (1, 17) | <0.001 |
| Predicted log-transformed ECV ($cm^3$) ~ Observed log-transformed ECV ($cm^3$) | $y = 2.00x - 3.37$ | 0.81 | 52.21 (1, 12) | <0.001 |
| Predicted PGR (from XMMC) ~ Predicted PGR (from ECV [$cm^3$]) | $y = 1.92x - 11.66$ | 0.82 | 53.33 (1, 12) | <0.001 |
| Predicted PGR (from ECV [$cm^3$]) ~ Geologic age | $y = -0.80x + 10.2352$ | 0.69 | 26.70 (1, 12) | <0.001 |
| Predicted PGR (from XMMC) ~ Geologic age | $y = -1.40x + 7.7353$ | 0.46 | 10.42 (1, 12) | <0.01 |

XMMC, maxillary MMC. All $P$ values are significant. PGLS $R^2$ and $P$ values are equivalent to the linear modeling results and are reported in *SI Appendix*, Table S6. PGR is calculated as the mass of the newborn (g) divided by the length of gestation (days); see *Materials and Methods* for more details.

**Table 2. Extant and fossil data used in this study, including average maxillary MMC values, observed PGRs and ECVs, and predicted PGRs and ECVs***

| Species | Average geologic age (Ma) | Average maxillary MMC | Observed PGR | Average predicted PGR (ECV) | Average predicted PGR (MMC) | Observed ECV ($cm^3$) | Observed logECV ($cm^3$) | Average predicted logECV ($cm^3$) |
|---|---|---|---|---|---|---|---|---|
| *Cercocebus torquatus* | Extant | 1.06 | 3.10 | — | — | 93.48 | 1.97 | — |
| *Cercopithecus mitis* | Extant | 0.95 | 2.90 | — | — | 65.62 | 1.82 | — |
| *Chlorocebus aethiops* | Extant | 0.96 | 1.94 | — | — | 58.25 | 1.77 | — |
| *Colobus guereza* | Extant | 1.08 | 2.63 | — | — | 72.00 | 1.86 | — |
| *Erythrocebus patas* | Extant | 1.04 | 3.72 | — | — | 87.57 | 1.94 | — |
| *Gorilla gorilla* | Extant | 1.00 | 8.16 | — | — | 433.74 | 2.64 | — |
| *Homo sapiens* | Extant | 0.84 | 11.58 | — | — | 1478.00 | 3.17 | — |
| *Lophocebus albigena* | Extant | 0.98 | 2.73 | — | — | 90.64 | 1.96 | — |
| *Macaca fascicularis* | Extant | 1.12 | 2.00 | — | — | 60.93 | 1.78 | — |
| *Mandrillus sphinx* | Extant | 1.15 | 3.52 | — | — | 136.42 | 2.13 | — |
| *Nasalis larvatus* | Extant | 1.09 | 2.73 | — | — | 84.85 | 1.93 | — |
| *Pan paniscus* | Extant | 0.93 | 5.95 | — | — | 326.25 | 2.51 | — |
| *Pan troglodytes* | Extant | 0.92 | 7.54 | — | — | 357.71 | 2.55 | — |
| *Papio hamadryas* | Extant | 1.22 | 4.94 | — | — | 137.00 | 2.14 | — |
| *Pongo pygmaeus* | Extant | 0.88 | 6.34 | — | — | 339.56 | 2.53 | — |
| *Semnopithecus entellus* | Extant | 1.06 | 2.60 | — | — | 95.24 | 1.98 | — |
| *Theropithecus gelada* | Extant | 1.25 | 2.60 | — | — | 123.22 | 2.09 | — |
| *Trachypithecus obscurus* | Extant | 1.03 | 2.07 | — | — | 59.30 | 1.77 | |
| *Ardipithecus ramidus* | 5.20 | 1.05 | — | 6.71 | 2.75 | 325.00 | 2.51 | 1.91 |
| *Australopithecus anamensis* | 4.05 | 1.04 | — | 7.09 | 2.80 | 370.00 | 2.57 | 1.92 |
| *Australopithecus afarensis* | 3.09 | 1.06 | — | 7.63 | 2.64 | 445.80 | 2.65 | 1.90 |
| *Australopithecus africanus* | 2.80 | 1.09 | — | 7.74 | 2.47 | 462.33 | 2.66 | 1.87 |
| *Homo ergaster* | 1.73 | 0.97 | — | 9.35 | 4.23 | 800.67 | 2.90 | 2.13 |
| *Homo habilis* | 1.69 | 0.98 | — | 8.55 | 4.02 | 610.00 | 2.79 | 2.10 |
| *Australopithecus boisei* | 1.63 | 1.00 | — | 8.06 | 3.50 | 515.00 | 2.71 | 2.02 |
| *Australopithecus robustus* | 1.50 | 1.12 | — | 7.93 | 2.46 | 493.33 | 2.69 | 1.88 |
| *Homo erectus* | 0.89 | 0.84 | — | 9.83 | 9.43 | 941.44 | 2.97 | 2.95 |
| *Homo heidelbergensis* | 0.47 | 0.79 | — | 10.70 | 11.77 | 1265.75 | 3.10 | 3.32 |
| *Homo naledi* | 0.29 | 1.00 | — | 8.01 | 3.50 | 507.50 | 2.71 | 2.02 |
| *Homo neanderthalensis* | 0.09 | 0.85 | — | 11.17 | 8.56 | 1487.50 | 3.17 | 2.81 |
| *Homo sapiens* (North Africa) | 0.07 | 0.86 | — | 10.84 | 8.45 | 1330.00 | 3.12 | 2.79 |
| *Homo sapiens* (South Africa) | 0.07 | 0.85 | — | 10.84 | 8.93 | 1330.00 | 3.12 | 2.87 |

Ma, millions of years ago; logECV, log-transformed ECV. Fossil ECVs and geologic ages are from (76, 98, 116, 117). *SI Appendix*, Table S1 includes minimum and maximum predicted values. PGR is calculated as the mass of the newborn (g) divided by the length of gestation (days); see *Materials and Methods* for more details.

modern humans (PGR ≈ 11 g/day). Overall, our model predicting PGR from fossil ECV finds that human-like PGR first evolved in later *Homo* ~0.25–0.75 million years ago.

Given the tight correlation between ECV and PGR in extant catarrhines, estimating PGR from fossil ECV (measured from fossil crania) is currently the best-supported method for predicting PGR in the fossil record (Fig. 1*B*). However, we also demonstrated that molar proportions are significantly correlated with PGR ($R^2 = 0.5$, $P = 0.004$; Fig. 2*A*) and ECV ($R^2 = 0.57$, $P = 0.001$; Fig. 2*B*) in extant catarrhines, offering a secondary method for estimating PGR in the fossil record. With these two methods, partial cranial and dental fossils can independently be used to predict PGRs in the fossil record.

**Molar Proportions Predict Increasing PGRs and ECVs in the Fossil Record.** Molar proportions (as captured by MMC) are significantly correlated with PGR and ECV in extant catarrhines (Fig. 2). We found a polynomial relationship to be the best fit for the data, largely because of the high MMC and PGR in baboons (*Papio hamadryas*). *Papio* is the most prognathic genus of the catarrhines, with notably elongated third molars. Among the extant catarrhines sampled, there is substantial overlap between species with approximately equal-length third and first molars (MMC ≈ 1). However, no species with an MMC >1 has a PGR >5, and no species with an MMC <1 has a PGR <5, a pattern that is emulated in our predictions of PGR. Building from the significant correlations in extant primates, we generated a polynomial regression model to predict PGRs from molar proportions in fossil hominids (Fig. 2*C*). Because PGR and ECV are so tightly correlated, we also predicted ECV from molar proportions in fossil hominids and compared our predictions to previously published ECVs reconstructed from fossil crania (77). This comparison of predicted versus observed ECVs serves as a model validation. Our predicted ECVs were significantly correlated with observed ECVs ($R^2 = 0.81$, $P < 0.001$; Table 1), demonstrating that our model predicts ECVs that are consistent with those estimated directly from cranial fossil remains (*SI Appendix*, Fig. S1*A*). Since our models are currently the only quantitative method for predicting PGRs in the fossil record, we were not able to compare our estimates with observed values. However, the tight correlation between ECV and PGR in extant taxa strongly suggests that our model reliably predicts PGR in the fossil record. Future studies that investigate life history, brain size, and molar proportions more broadly across primates may help elucidate the ecological and physiological pressures shaping the associations between these traits.

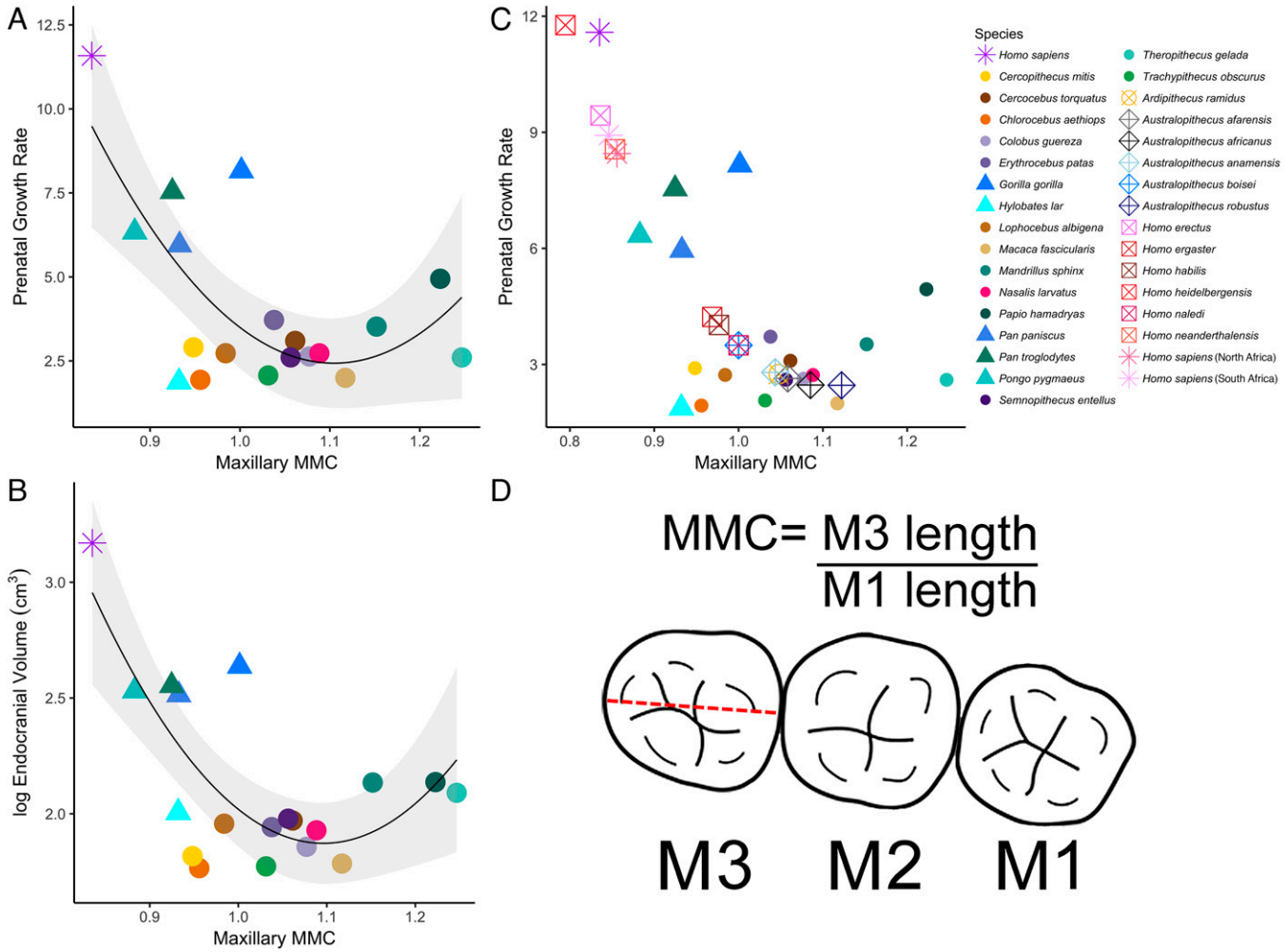


**Fig. 2.** (*A*) PGRs ($R^2$ = 0.50, $P$ < 0.004) and (*B*) log-transformed ECVs ($R^2$ = 0.57, $P$ = 0.001) are significantly correlated with maxillary MMC in extant catarrhines. (*C*) PGRs of fossil hominids, reconstructed from molar proportions, are plotted alongside extant catarrhines. Values were reconstructed via a linear regression model developed from extant data (Table 1). (*D*) Figurative illustration of MMC in apes. Dashed red line on the third molar (M3) indicates where molar mesiodistal length is measured. Distal is to the *Left*, and mesial is to the *Right*. *Homo sapiens* are labeled with an asterisk, extant cercopithecids are labeled with a circle, extant nonhuman apes are labeled with a triangle, *Ardipithecus* is marked with a crossed circle, *Australopithecus* are marked with a crossed diamond, and nonhuman fossil *Homo* species are marked with a crossed square. *Homo sapiens* (North Africa) and (South Africa) are fossil samples. *SI Appendix*, Figs. S3 and S4 include mandibular MMC results.

Consistent with our findings from ECV, our dental model predicts lower PGRs for *Ardipithecus*, *Australopithecus*, and early *Homo*, similar to values seen in extant cercopithecids and nonhuman apes. This model predicts that PGR first increased beyond rates seen in extant nonhuman apes (PGR >8) ~1–1.5 million years ago with *H. erectus*, and further increased in the geologically more recent *H. heidelbergensis*, *H. neanderthalensis*, and fossil *H. sapiens*. Both models support significantly increasing PGRs throughout the terminal Miocene and Plio-Pleistocene, with predicted PGR significantly correlated with geologic time in fossil hominids ($P$ < 0.01 for predictions from ECV and MMC; Table 1 and *SI Appendix*, Fig. S2 *A* and *B*).

Additionally, we found that the predictions of PGR from fossil ECV values are significantly correlated with the predictions of PGR from maxillary dental proportions ($R^2$ = 0.82, $P$ < 0.001; Table 1 and *SI Appendix*, Fig. S1*B*). Because several of the extant species sampled have proportionately equal third and first molar lengths (MMC ~1), the dental model underpredicts PGR at higher MMC values (MMC >0.9). However, predictions at lower MMC values (MMC <0.9) have smaller confidence intervals and more closely approximate predictions from ECV (*SI Appendix*, Table S1). Overall, the predictions from this model are significantly correlated with predictions derived from the ECV model. While ECV is a more statistically supported predictor of PGR in fossil hominids, predictions from molar proportions are still strongly and significantly supported (correlated with observed ECV values, $P$ < 0.001; correlated with predictions from ECV model, $P$ < 0.001). Both models support increasing PGR over the last 6 million years, with human-like PGRs (>9.87 g/day) first evolving within the last 1 million years in later *Homo*.

## Discussion

We demonstrated that PGR can be reconstructed in the hominid fossil record by using fossilized cranial and dental remains. The results from both methods are significantly correlated: Both models indicate that PGR has increased significantly over the last 6 million years, and both models indicate that a human-like PGR (i.e., more similar to humans than to other extant apes) first evolved in later *Homo*, about 0.5 million years ago (0.25–0.75 Ma). Synthesizing the predictions from both models, we found evidence that increases in PGR during hominid evolution align with major taxonomic and morphological changes, as seen in many aspects of hominid biology.

**Evolution of PGRs in Hominid Evolution.** Our statistically supported predictions of PGR broadly reflect anatomical and evolutionary changes across geologic time (Fig. 3) and align with previous work on the evolution of neonatal brain size and pelvic morphology in hominids (19, 20, 28, 72, 78). Fossil evidence from the Late Miocene and Early Pliocene first reflects a shift in locomotor habitus, with adaptations to bipedality visible in the skeletons of *Ardipithecus*, and especially *Australopithecus* (79, 80).

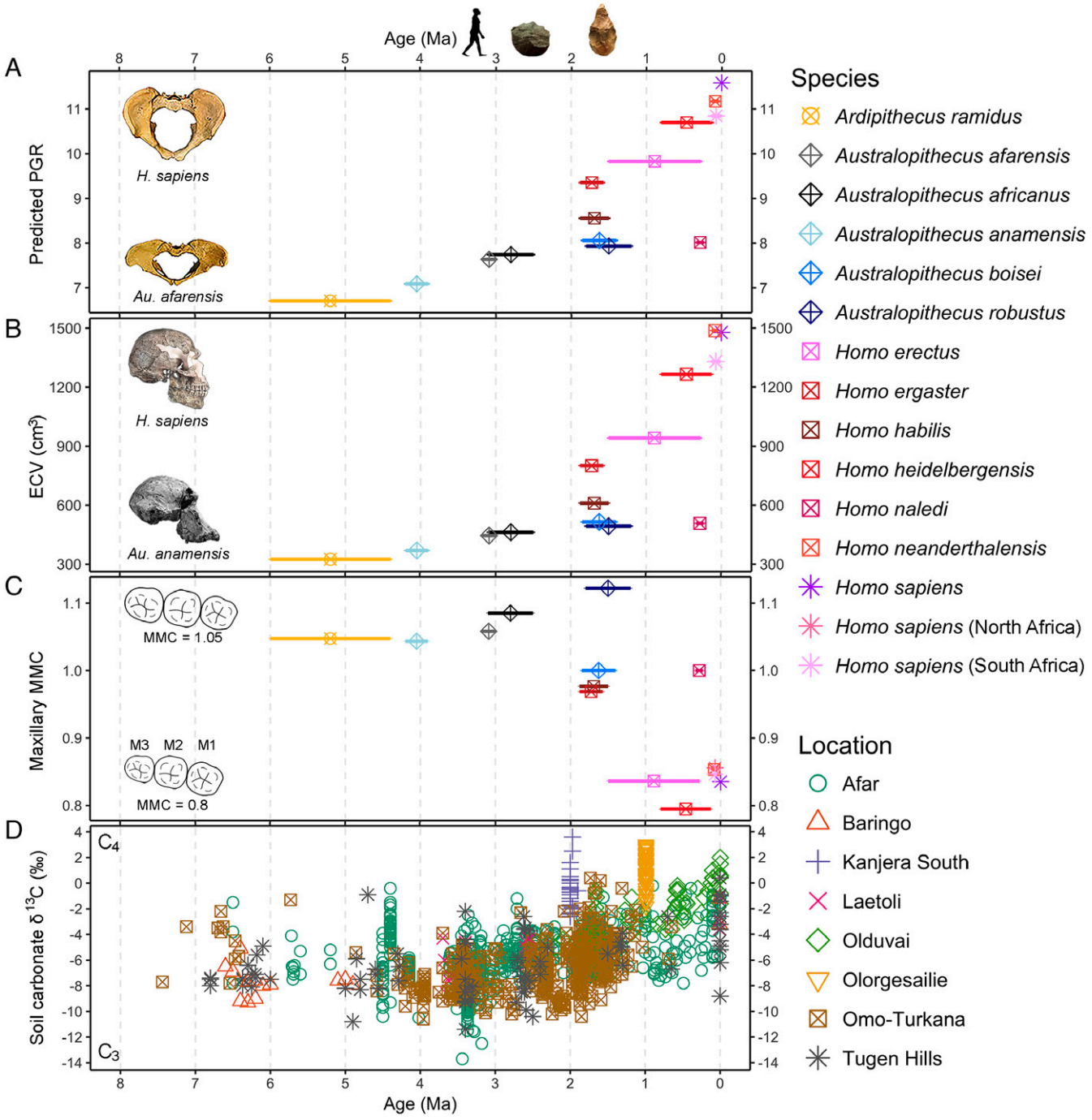


**Fig. 3.** Timeline of morphological, behavioral, and ecological changes in the hominid fossil record from terminal Miocene to present. The *x*-axis is geologic time in millions of years (Ma). The *y*-axes are parsed by variable. From *Top* to *Bottom*: (*A*) Predicted PGR, predicted via the linear regression model (for ECV) developed as part of the method published in this article. (*B*) ECV (in cubic centimeters) reconstructed from cranial fossil specimens [data from (77)]. (*C*) Maxillary MMC. (*D*) Soil carbonate $\delta^{13}C$ (‰ Vienna Pee Dee Belemnite), sampled from paleosols in eastern African hominid-bearing areas. Stable isotope data (*D*) were obtained from (101); temporal shifts toward more positive (enriched) isotopic values on the *y*-axis indicate ecological transitions from $C_3$ to $C_4$ vegetation coinciding with climatological increases in aridity. Fossil species are plotted as averages with error bars to represent currently known first and last appearance dates (77, 97, 116, 117). Evolutionary changes in pelvic shape, ECV, and MMC are visualized through extremes (*A*–*C*, respectively). PGR is represented by fossil pelves from *Australopithecus afarensis* AL 288-1 and recent *Homo sapiens* [images adapted from (118)]. ECV is represented by *Australopithecus anamensis* MRD-VP-1/1 [image adapted from (116)] and *Homo sapiens* Skhul V [image adapted from (119)]. MMC is represented by a figurative visualization of dental proportions. Major changes in behavior are plotted on the *x*-axis at the top of the figure using illustrative images, representing the evolution of obligate bipedalism, use of Oldowan tools, and use of Acheulean tools [images and dates are adapted from (75)]. Figure legend includes fossil taxa and extant *Homo sapiens*. Fossil *Homo sapiens* are demarcated as North Africa and South Africa. *Location* refers to the sites where the soil carbonate isotopes were sampled. *SI Appendix*, Fig. S8 includes expanded figure that includes PGR predicted from MMC, and additional stable isotope data.

During this period, *Ardipithecus* and *Australopithecus* are predicted to have had lower PGRs and smaller ECVs, more similar to those of extant monkeys and apes today, as well as third molars that are larger than, or approximately equal in size to, the first molars.

Our models indicate that PGRs increased about 1.5–2 million years ago alongside increasing brain size, a phenomenon associated with the evolution of genus *Homo*. Our method of predicting PGR from fossil ECV supports the interpretation that PGR first exceeded what is seen in extant apes today during this period of the Early Pleistocene. However, early *Homo*, including *H. ergaster* and *H. habilis*, are predicted to have had PGRs and ECVs that were still more similar to those of extant apes than modern humans (PGR <9.87 g/day). The predictions of PGR from the dentition are lower but still reflect an increase from what is predicted for early hominids, as well as a lower predicted PGR than in later *Homo*. There is also a reduction of the third molar relative to the first molar (lower MMC). The behavioral evidence from this period demonstrates refinements in tool making, perhaps reflecting a cognitive shift that enabled the imposition of preconceived form onto stone (81). While there is some evidence for butchery as early as 2.5 million years ago (82), or perhaps even 3.3 million years ago (83), advanced food processing behavior became much more common during this later phase (84) and may have supported the substantial calorie intake required for the evolution of increased brain size (17). Other hypothesized factors in increasing brain size include changes in social structure and metabolic physiology (85).

Hominid PGRs increased substantially again with the evolution of *H. erectus* in the Early Pleistocene (Fig. 3). An increased PGR occurs in step with increasing brain size in *H. erectus* and may be associated with, if not driving, the evolution of increasing encephalization in Pleistocene hominids (86). This may have occurred in tandem with increases in metabolic rate, which are hypothesized to be a strong driver in the evolution of brain size and life history in humans (17). Near this time, the fossil and archaeological records demonstrate notable increases in the production and use of technology, as well as the first near-global dispersal of a hominid species (87). The fossil evidence also indicates that, alongside increases in brain size, human-like limb proportions first evolved in *H. erectus* (88). The pelvic anatomy of *H. erectus* has been suggested to demonstrate evidence for a high PGR similar to that of humans, but other researchers have cautioned against an overreliance on pelvic anatomy for reconstructing life history traits such as prenatal or postnatal growth rates (76, 88–91). This ongoing debate further emphasizes the importance of the methods described herein. Taken together, these changes in bony anatomy reinforce our predictions of a high PGR in *H. erectus* and support the interpretation that metabolically costly pregnancy and difficult birth evolved in Pleistocene *Homo*.

Research on Neanderthal pelvic and perinatal cranial dimensions supports a rotational, or at least very difficult, birth in this taxon, much like that of modern humans (20, 92). Fossil evidence also supports a rotational birth in later *Homo*, including *H. erectus* in the Middle Pleistocene (93). This is in line with Walker and Ruff's (88) conclusions that *H. erectus* had a neonatal brain size and pelvic canal diameter similar to that of modern humans, resulting in a difficult, rotational delivery. In contrast, reconstructions of *Australopithecus sediba* pelvic anatomy support a nonrotational birth in this geologically older taxon, with no evidence for cranial or shoulder constraints in the birth canal (94). Our predictions for PGR align with this previous research in supporting a human-like PGR (>9.87 g/day) and ECV in later *Homo*, evolving in *H. heidelbergensis* ~0.25–0.75 million years ago. Changing pelvic anatomy, endocranial volume, and predicted PGRs all provide independent lines of evidence that support human-like pregnancy and birth evolving in the Pleistocene in the later *Homo* species, before the emergence of *Homo sapiens* (Fig. 3).

Our research provides a line of evidence for an increase in PGRs over the last 6 million years. We found a statistically significant relationship between predicted PGR and geologic time for both the cranial and dental models. One exception is seen with *H. naledi*. The *H. naledi* predicted PGR falls in between the *Ardipithecus*/*Australopithecus* and early *Homo* clades, as would be expected given the similar molar proportions and ECV (Table 2), but in contrast to the young geologic age estimated for this taxon (95). This affinity to early *Homo* is not particularly surprising as it echoes other reports of mosaic anatomy in *H. naledi*, comprising a mix of ancestral and derived features [including in dental morphology (66, 96–98)]. Our data indicate that *H. naledi* had the lowest PGR of all species in genus *Homo*, more similar to *Australopithecus boisei* and extant apes today.

## Conclusions

We detailed and quantitatively validated two methods for reconstructing PGRs from primate skeletal materials: predictions based on endocranial volume and predictions based on molar proportions. Together with previous work on African ecology (from paleosol and tooth isotope data), as well as dental, pelvic, and endocranial morphology, our reconstructed PGRs build a picture of increasing maternal energetics during pregnancy over the last 6 million years of hominid evolution. Expanding $C_4$ grasslands and herbivore populations coincide with evolutionary advancements in tool technologies and evolutionary increases in brain size in genus *Homo* (99). These changes may have provided the impetus for the increased resource provisioning necessary for growing prenatal and postnatal infant brains (25, 100–102). Increased neonatal size and maternal investment have also been hypothesized to be linked to locomotion and selection on bipedality (30). These increases can be further associated with behaviors linked to changes in social structure and larger group sizes (32), including the likely evolution of group hunting and early language (103). Together, the data support a changing morphological and ecological landscape of increased resources available to gestating mothers, as well as to their helpless infants. This feedback loop may have in turn allowed for the evolution of even larger brains and increased cranial capacity in later *Homo*, leading to *H. sapiens.*

## Materials and Methods

**Extant Materials.** PGR is an informative trait that quantifies growth of the fetus and maternal energetics. Using data for 19 extant catarrhine primate species, we demonstrated that adult ECV is a very strong predictor of PGR ($R^2 = 0.93$; Fig. 1*A*). Our previous work on platyrrhines (59) hypothesized that PGR is tied to molar development, including size and number. This provided the theoretical basis for our hypothesis that postcanine tooth proportions are correlated with PGR in primates.

We measured the molar dentition for 608 catarrhine primates across 18 extant species and collected data for gibbons from the literature ($n = 1$) to assess the quantitative relationship between the postcanine dentition, PGR, and ECV (Tables 1 and 2). Dental metrics were taken with calipers according to published standards (104). Our growing body of work has demonstrated that molar proportions (MMC) are heritable, have a reliable phylogenetic signal, and are independent of diet and body size (57, 65–69). For this study, we focused on

relative third molar length, as captured by the MMC. We focused on third molar proportions because they are an evolutionarily and morphologically interesting trait in humans (52, 64), and because our previous work hypothesized that PGRs are linked to third molar presence through the iterative developmental processes of postcanine tooth development (59). We statistically compared third molar proportions (MMC), PGR, and ECV in extant catarrhines, controlling for phylogenetic relatedness by using phylogenetic generalized least squares regression (PGLS). Our extant analyses focused on catarrhine species ($n = 19$) for which we had postcanine dental data, PGR (grams/day), ECV (cubic centimeters), and molecular data. Dental proportions were averaged from 608 primate individuals across 18 species and combined with data for gibbons from the literature (105) (see *SI Appendix*, Table S4 for species sample sizes and Table 2 for average trait values by species).

Dental data were collected as linear dental metrics. MMC was calculated with the following equation according to previous standards for the trait (57):

$$MMC = \frac{Mesiodistal\ length\ of\ the\ third\ molar}{Mesiodistal\ length\ of\ the\ first\ molar}.$$

We calculated both maxillary and mandibular MMC from our linear metric data for analyses. The maxillary data had stronger statistical fit with PGRs and ECVs in extant primates, probably related to the variable presence of the hypoconulid on the lower third molar in catarrhines (106). Therefore, we present the maxillary data in the main body of the article. Results from the mandibular data are still significant and are presented in the *SI Appendix*. Residual plots from models of linear regressions between PGR and maxillary MMC, log-transformed ECV and maxillary MMC, and PGR and log-transformed ECV are reported in *SI Appendix*, Fig. S5.

Additionally, we calculated dental area to see whether it outperformed MMC as a predictor of published ECV values. Dental area was calculated as:

$$Tooth\ area = Mesiodistal\ tooth\ length \times Buccolingual\ tooth\ width.$$

We used size-corrected (square root) tooth area for all tooth area analyses (*SI Appendix*, Table S5). Results for maxillary and mandibular tooth area are available in *SI Appendix*, Figs. S6 and S7.

Average PGR and ECV were used for each extant species. PGR was calculated according to previous standards (22) and the following equation:

$$Prenatal\ growth\ rate = \frac{Neonatal\ birth\ weight\ (grams)}{Gestation\ length\ (days)}.$$

Neonatal birth weight and gestation length were taken from (22) for all species except *Chlorocebus aethiops*, *Trachypithecus obscurus*, and *Semnopithecus entellus*; data for these species were compiled from the online life history database AnAge, part of the Human Aging Genomic Resources database (107). All ECV averages for extant primates were taken from (108).

To test the fossil applications of this method, we compiled data on molar proportions for 13 fossil species. After testing for the effects of phylogeny via PGLS, we generated a linear regression equation from the extant catarrhines and applied it to our fossil data as a predictive model. As another quality check on our model, we compiled data on reconstructed ECV for all 13 fossil species (detailed below).

**Fossil Materials.** We used previously published dental data for all fossils included in our analyses [majority of data from (98); see *SI Appendix* for details]. We also gathered published ECVs (cubic centimeters) for the fossils included in our dataset (77). These ECVs were compiled from other publications that made estimates directly from cranial fossil specimens. With these fossil data, we predicted ECV using our molar proportion method and compared it to the published ECV reconstructions (Table 1). For consistency with the adaptive grade-based definition of the human clade used in our previous work, we use *Hominidae* (and *hominid*) to refer to all taxa on the human side of the human–chimpanzee divergence.

**Statistical Analyses.** Statistical analyses and figures were produced in R version 4.1.2 (109) via RStudio software version 2021.09.1+372 (110). All plots were made with the *ggplot2* package (111), and averages and log-transformed values were calculated with the *dplyr* package (112).

To statistically test the relationships between PGR, ECV, and MMC in extant catarrhines, we conducted a PGLS regression analysis by using a published phylogenetic supertree built from molecular data and generated via a heuristic-hierarchical Bayesian method (113). We read and truncated the phylogenetic tree using *ape* (114). The PGLS analysis was run with the pgls function in *caper* (115). After testing for the effect of phylogeny with PGLS, we used the lm function in R to build models describing the statistical relationship between each pair of traits. A linear model for the relationship between PGR and ECV was most significantly supported via PGLS and lm. Quadratic polynomial models were most significantly supported via PGLS and lm for the relationship between PGR and maxillary MMC and between ECV and maxillary MMC (lm models reported in Table 1; PGLS models reported in *SI Appendix*, Table S6). The lm models were then used to predict PGR and ECV for hominid fossils (see Table 1 for model equations and Table 2 for predicted values).

We visualized predicted PGRs in hominids by plotting predicted PGRs against fossil ECV and maxillary MMC values and including observed PGRs for extant species from the literature (Figs. 1*B* and 2*C*). As a check of our model validity, we also compared predicted ECV (from our polynomial regression model) with observed ECV (from fossil cranial data) across the sampled hominids. Predicted and observed ECVs are significantly correlated, indicating that our regression model successfully predicts ECV in a way that accords with observed values from fossil crania (*SI Appendix*, Fig. S1*A*). Our predicted ECV values are lower than the observed ECV values, but they are significantly correlated. The difference between predicted and observed values could be related to underestimation in our dental model. The PGR predictions generated from the ECV and dental models are significantly correlated ($R^2 = 0.82$, $P < 0.001$). All results for mandibular MMC are presented in the *SI Appendix*. All original maxillary dental data collected for this study, and all R code used to conduct analyses, are available at https://github.com/teslamonson/prenatal. Mandibular dental data are from a previously published dataset (57).

**Data, Materials, and Software Availability.** Dental measurement data have been deposited in GitHub (https://github.com/teslamonson/prenatal). All study data are included in the article and/or supporting information. Previously published data were used for this work [1. L. J. Hlusko, C. A. Schmitt, T. A. Monson, M. F. Brasil, M. C. Mahaney. The integration of quantitative genetics, paleontology, and neontology reveals genetic underpinnings of primate dental evolution. Proc. Natl. Acad. Sci. U.S.A. 113(33), 9262–9267 (2016). 2. R. L. Holloway, D. C. Broadfield, M. S. Yuan. The Human Fossil Record, Brain Endocasts-The Paleoneurological Evidence (John Wiley and Sons, 2004). 3. S. H. Montgomery, N. I. Mundy. Parallel episodes of phyletic dwarfism in callitrichid and cheirogaleid primates. J. Evol. Biol. 26(4), 810–819 (2013). 4. R. Tacutu, T. Craig, A. Budovsky, D. Wuttke, G. Lehmann, D. Taranukha,... J. P. de Magalhães. Human aging genomic resources: Integrated databases and tools for the biology and genetics of aging. Nuc. Acids. Res. 41, D1027–D1033 (2012). 5. P. W. Lucas, R. T. Corlett, D. A. Luke. Postcanine tooth size and diet in anthropoid primates. Z. Morph. Anthropol. 76(3), 253–276 (1986). 6. J. D. Irish, M. Grabowski. Relative tooth size, Bayesian inference, and *Homo naledi*. Am. J. Phys. Anthropol. 176(2), 262–282 (2021). 7. Y. Haile-Selassie, S. M. Melillo, A. Vazzana, S. Benazzi, T. M. Ryan. A 3.8-million-year-old hominin cranium from Woranso-Mille, Ethiopia. Nature 573(7773), 214–219 (2019). 8. G. Suwa, R. T. Kono, S. W. Simpson, B. Asfaw, C. O. Lovejoy, T. D. White. Paleobiological implications of the *Ardipithecus ramidus* dentition. Science, 326(5949), 69–99 (2009). 9. R. L. Holloway, S. D. Hurst, H. M. Garvin, P. T. Schoenemann, W. B. Vanti, L. R. Berger, J. Hawks. Endocast morphology of *Homo naledi* from the Dinaledi Chamber, South Africa. Proc. Natl. Acad. Sci. U.S.A. 115(22), 5738–5743 (2018). 10. Y. Kaifu, R. T. Kono, T. Sutikna, E. W. Saptomo, R. A. Due. Unique dental morphology of *Homo floresiensis* and its evolutionary implications. PloS One 10(11), e0141614 (2015). 11. D. Kubo, R. T. Kono, Y. Kaifu. Brain size of *Homo floresiensis* and its evolutionary implications. Proc. Roy. Soc. B 280(1760), 20130338 (2013). 12. L. E. Powell, K. Isler, R. A. Barton. Re-evaluating the link between brain size and behavioral ecology in primates. Phil. Trans. Roy. Soc. B 284(1865), 20171765 (2017)].

**ACKNOWLEDGMENTS.** The authors thank curators at the following museums for facilitating access to collections: American Museum of Natural History in New York City, Anthropology Museum at University of Zurich, Cleveland Museum of Natural History in Ohio, Museum of Vertebrate Zoology and Phoebe A. Hearst Museum of Anthropology at University of California Berkeley, and Smithsonian's National Museum of Natural History in Washington, DC. The authors also thank Gen Suwa and Tim White for providing extant hominoid dental data. A.P.W. was

supported by the Washington Research Foundation, and M.F.B. was supported by the John Templeton Foundation for the duration of this research. Much of the data collection for the extant primates was funded by National Science Foundation Division of Behavioral and Cognitive Sciences grants 0500179, 0616308, and 0130277 to L.J.H.

Author affiliations: [a]Department of Anthropology, Western Washington University, Bellingham, WA 98225; [b]Department of Environmental Sciences, Western Washington University, Bellingham, WA 98225; [c]Berkeley Geochronology Center, Berkeley, CA, 94709; [d]Human Evolution Research Center, University of California, Berkeley, CA 94720; [e]Centro Nacional de Investigación sobre la Evolución Humana, Burgos, Spain 09002; and [f]Department of Integrative Biology, University of California, Berkeley, CA 94720


1. W. Dirks, J. E. Bowman, Life history theory and dental development in four species of catarrhine primates. *J. Hum. Evol.* **53**, 309–320 (2007).
2. S. R. Leigh, G. E. Blomquist, "Life history" *in Primates in Perspective*, C. J. Campbell, A. Fuentes, K. C. MacKinnon, M. Panger, S. K. Beader, Eds. (Oxford University Press, 2007), pp. 396–407.
3. R. Gowland, S. Halcrow, *The Mother-Infant Nexus in Anthropology* (Springer, 2020).
4. J. M. DeSilva, J. J. Lesnik, Brain size at birth throughout human evolution: A new method for estimating neonatal brain size in hominins. *J. Hum. Evol.* **55**, 1064–1074 (2008).
5. H. M. Dunsworth, A. G. Warrener, T. Deacon, P. T. Ellison, H. Pontzer, Metabolic hypothesis for human altriciality. *Proc. Natl. Acad. Sci. U.S.A.* **109**, 15212–15216 (2012).
6. R. I. M. Dunbar, *Primate Social Systems* (Springer Science & Business Media, 2013).
7. W. R. Trevathan, K. R. Rosenberg, Eds., *Costly and Cute: Helpless Infants and Human Evolution* (University of New Mexico Press, 2016).
8. C. P. van Schaik, R. Dunbar, The evolution of monogamy in large primates: A new hypothesis and some crucial tests. *Behav.* **115**, 30–61 (2016).
9. J. Allman, T. McLaughlin, A. Hakeem, Brain weight and life-span in primate species. *Proc. Natl. Acad. Sci. U.S.A.* **90**, 118–122 (1993).
10. A. R. DeCasien, N. A. Thompson, S. A. Williams, M. R. Shattuck, Encephalization and longevity evolved in a correlated fashion in Euarchontoglires but not in other mammals. *Evolution* **72**, 2617–2631 (2018).
11. R. I. Dunbar, S. Shultz, Evolution in the social brain. *Science* **317**, 1344–1347 (2007).
12. S. Elton, L. C. Bishop, B. Wood, Comparative context of Plio-Pleistocene hominin brain evolution. *J. Hum. Evol.* **41**, 1–27 (2001).
13. M. González-Forero, A. Gardner, Inference of ecological and social drivers of human brain-size evolution. *Nature* **557**, 554–557 (2018).
14. S. A. Heldstab, K. Isler, J. M. Burkart, C. P. van Schaik, Allomaternal care, brains and fertility in mammals: Who cares matters. *Behav. Ecol. Sociobiol.* **73**, 1–13 (2019).
15. R. D. Martin, Scaling of the mammalian brain: The maternal energy hypothesis. *Physiology* **11**, 149–156 (1996).
16. A. Navarrete, C. P. van Schaik, K. Isler, Energetics and the evolution of human brain size. *Nature* **480**, 91–93 (2011).
17. H. Pontzer *et al.*, Metabolic acceleration and the evolution of human brain size and life history. *Nature* **533**, 390–392 (2016).
18. H. Coqueugniot, J. J. Hublin, F. Veillon, F. Houët, T. Jacob, Early brain growth in *Homo erectus* and implications for cognitive ability. *Nature* **431**, 299–302 (2004).
19. J. M. DeSilva, J. J. Lesnik, Chimpanzee neonatal brain size: Implications for brain growth in *Homo erectus*. *J. Hum. Evol.* **51**, 207–212 (2006).
20. M. S. Ponce de León *et al.*, Neandertal brain size at birth provides insights into the evolution of human life history. *Proc. Natl. Acad. Sci. U.S.A.* **105**, 13764–13768 (2008).
21. K. Isler, C. P. van Schaik, The Expensive Brain: A framework for explaining evolutionary changes in brain size. *J. Hum. Evol.* **57**, 392–400 (2009).
22. S. H. Montgomery, N. I. Mundy, Parallel episodes of phyletic dwarfism in callitrichid and cheirogaleid primates. *J. Evol. Biol.* **26**, 810–819 (2013).
23. P. H. Harvey, T. H. Clutton-Brock, Life history variation in primates. *Evolution* **39**, 559–581 (1985).
24. C. Ross, Primate life histories. *Evol. Anthropol.* **6**, 54–63 (1998).
25. Z. Cofran, J. M. DeSilva, A neonatal perspective on *Homo erectus* brain growth. *J. Hum. Evol.* **81**, 41–47 (2015).
26. S. R. Leigh, Brain growth, life history, and cognition in primate and human evolution. *Am. J. Primatol.* **62**, 139–164 (2004).
27. N. Roelfsema, W. Hop, S. Boito, J. Wladimiroff, Three-dimensional sonographic measurement of normal fetal brain volume during the second half of pregnancy. *Am. J. Obstet. Gynecol.* **190**, 275–280 (2004).
28. S. R. Leigh, Brain ontogeny and life history in *Homo erectus*. *J. Hum. Evol.* **50**, 104–108 (2006).
29. B. H. Smith, R. L. Tompkins, Toward a life history of the Hominidae. *Annu. Rev. Anthropol.* **24**, 257–279 (1995).
30. J. M. DeSilva, A shift toward birthing relatively large infants early in human evolution. *Proc. Natl. Acad. Sci. U.S.A.* **108**, 1022–1027 (2011).
31. A. Nowell, H. Kurki, "Moving beyond the obstetrical dilemma hypothesis: Birth, weaning and infant care in the Plio-Pleistocene" in *The Mother-Infant Nexus in Anthropology*, R. Gowland, S. Halcrow, Eds. (Springer, 2020), pp. 173–190.
32. R. I. Dunbar, The social brain hypothesis and its implications for social evolution. *Ann. Hum. Biol.* **36**, 562–572 (2009).
33. J. M. Burkart, S. B. Hrdy, C. P. Van Schaik, Cooperative breeding and human cognitive evolution. *Evol. Anthropol.* **18**, 175–186 (2009).
34. S. B. Hrdy, "Evolutionary context of human development: The cooperative breeding model" in *Family Relationships: An Evolutionary Perspective*, C. A. Salmon, T. K. Shackelford, Eds. (Oxford University Press, 2007), pp. 39–68.
35. S. B. Hrdy, *Mothers and Others: The Evolutionary Origins of Mutual Understanding* (Harvard University Press, 2009).
36. K. Isler, C. P. van Schaik, Allomaternal care, life history and brain size evolution in mammals. *J. Hum. Evol.* **63**, 52–63 (2012).
37. K. Isler, C. P. Van Schaik, How humans evolved large brains: Comparative evidence. *Evol. Anthropol.* **23**, 65–75 (2014).
38. J. C. Mitani, D. Watts, The evolution of non-maternal caretaking among anthropoid primates: Do helpers help? *Behav. Ecol. Sociobiol.* **40**, 213–220 (1997).
39. L. C. Aiello, P. Wheeler, The expensive-tissue hypothesis: The brain and the digestive system in human and primate evolution. *Curr. Anthropol.* **36**, 199–221 (1995).
40. J. J. Hublin, S. Neubauer, P. Gunz. Brain ontogeny and life history in Pleistocene hominins. *Philos. Trans. R. Soc. B* **370**, 20140062 (2015).
41. R. A. Barton, I. Capellini, Maternal investment, life histories, and the costs of brain growth in mammals. *Proc. Natl. Acad. Sci. U.S.A.* **108**, 6169–6174 (2011).
42. A. C. Halley, Minimal variation in eutherian brain growth rates during fetal neurogenesis. *Proc. R. Soc. B* **284**, 20170219 (2017).
43. K. A. Koffi *et al.*, The role of GH/IGF axis in dento-alveolar complex from development to aging and therapeutics: A narrative review. *Cells* **10**, 1181 (2021).
44. T. Yu, O. D. Klein, Molecular and cellular mechanisms of tooth development, homeostasis and repair. *Development* **147**, dev184754 (2020).
45. M. C. Dean, Tooth microstructure tracks the pace of human life-history evolution. *Proc. Biol. Sci.* **273**, 2799–2808 (2006).
46. G. A. Macho, Primate molar crown formation times and life history evolution revisited. *Am. J. Primatol.* **55**, 189–201 (2001).
47. B. H. Smith, Dental development as a measure of life history in primates. *Evolution* **43**, 683–688 (1989).
48. B. H. Smith, Dental development and the evolution of life history in Hominidae. *Am. J. Phys. Anthropol.* **86**, 157–174 (1991).
49. T. M. Smith, Teeth and human life-history evolution. *Annu. Rev. Anthropol.* **42**, 191–208 (2013).
50. T. M. Smith *et al.*, First molar eruption, weaning, and life history in living wild chimpanzees. *Proc. Natl. Acad. Sci. U.S.A.* **110**, 2787–2791 (2013).
51. S. R. Leigh, J. M. Setchell, M. Charpentier, L. A. Knapp, E. J. Wickings, Canine tooth size and fitness in male mandrills (*Mandrillus sphinx*). *J. Hum. Evol.* **55**, 75–85 (2008).
52. J. M. Bermúdez De Castro, A. Rosas, Pattern of dental development in Hominid XVIII from the Middle Pleistocene Atapuerca-Sima de los Huesos site (Spain). *Am. J. Phys. Anthropol.* **114**, 325–330 (2001).
53. M. C. Dean *et al.*, Growth processes in teeth distinguish modern humans from *Homo erectus* and earlier hominins. *Nature* **414**, 628–631 (2001).
54. L. R. Godfrey, K. E. Samonds, W. L. Jungers, M. R. Sutherland, Teeth, brains, and primate life histories. *Am. J. Phys. Anthropol.* **114**, 192–214 (2001).
55. D. Guatelli-Steinberg, D. J. Reid, T. A. Bishop, C. S. Larsen, Anterior tooth growth periods in Neandertals were comparable to those of modern humans. *Proc. Natl. Acad. Sci. U.S.A.* **102**, 14197–14202 (2005).
56. L. J. Hlusko, L. R. Lease, M. C. Mahaney, Evolution of genetically correlated traits: Tooth size and body size in baboons. *Am. J. Phys. Anthropol.* **131**, 420–427 (2006).
57. L. J. Hlusko, C. A. Schmitt, T. A. Monson, M. F. Brasil, M. C. Mahaney, The integration of quantitative genetics, paleontology, and neontology reveals genetic underpinnings of primate dental evolution. *Proc. Natl. Acad. Sci. U.S.A.* **113**, 9262–9267 (2016).
58. L. J. Hlusko *et al.*, Environmental selection during the last ice age on the mother-to-infant transmission of vitamin D and fatty acids through breast milk. *Proc. Natl. Acad. Sci. U.S.A.* **115**, E4426–E4432 (2018).
59. T. A. Monson, J. L. Coleman, L. J. Hlusko, Craniodental allometry, prenatal growth rates, and the evolutionary loss of the third molars in New World monkeys. *Anat. Rec. (Hoboken)* **302**, 1419–1433 (2019).
60. K. Carter, "The evolution of third molar agenesis and impaction," Doctoral dissertation, Harvard University (2016).
61. K. E. Carter, S. Worthington, The evolution of anthropoid molar proportions. *BMC Evol. Biol.* **16**, 110 (2016).
62. M. Scheiwiller, E. S. Oeschger, N. Gkantidis, Third molar agenesis in modern humans with and without agenesis of other teeth. *PeerJ* **8**, e10367 (2020).
63. J. M. Bermúdez de Castro, M. E. Nicolas, Posterior dental size reduction in hominids: The Atapuerca evidence. *Am. J. Phys. Anthropol.* **96**, 335–356 (1995).
64. B. Wood, Origin and evolution of the genus *Homo*. *Nature* **355**, 783–790 (1992).
65. T. A. Monson *et al.*, Keeping 21st century paleontology grounded: Quantitative genetic analyses and ancestral state reconstruction re-emphasize the essentiality of fossils. *Biology (Basel)* **11**, 1218 (2022).
66. M. F. Brasil, T. A. Monson, C. A. Schmitt, L. J. Hlusko, A genotype:phenotype approach to testing taxonomic hypotheses in hominids. *Naturwissenschaften* **107**, 40 (2020).
67. T. A. Monson, D. W. Armitage, L. J. Hlusko, Using machine learning to classify extant apes and interpret the dental morphology of the chimpanzee-human last common ancestor. *PaleoBios* **35**, 1–20 (2018).
68. T. A. Monson *et al.*, Evidence of strong stabilizing effects on the evolution of boreoeutherian (Mammalia) dental proportions. *Ecol. Evol.* **9**, 7597–7612 (2019).
69. M. E. Zuercher, T. A. Monson, R. R. Dvoretzky, S. Ravindramurthy, L. J. Hlusko, Dental variation in megabats (Chiroptera: Pteropodidae): Tooth metrics correlate with body size and tooth proportions reflect phylogeny. *J. Mamm. Evol.* **28**, 543–558 (2021).
70. E. Giabicani *et al.*, Increasing knowledge in *IGF1R* defects: Lessons from 35 new patients. *J. Med. Genet.* **57**, 160–168 (2020).
71. W. C. Hartwig, Ed., *The Primate Fossil Record* (Cambridge University Press, 2002), vol. 419.
72. S. L. Robson, B. Wood, Hominin life history: Reconstruction and evolution. *J. Anat.* **212**, 394–425 (2008).
73. T. M. Smith *et al.*, Earliest evidence of modern human life history in North African early *Homo sapiens*. *Proc. Natl. Acad. Sci. U.S.A.* **104**, 6128–6133 (2007).
74. T. M. Smith *et al.*, Dental evidence for ontogenetic differences between modern humans and Neanderthals. *Proc. Natl. Acad. Sci. U.S.A.* **107**, 20923–20928 (2010).
75. S. C. Antón, R. Potts, L. C. Aiello, Evolution of early *Homo*: An integrated biological perspective. *Science* **345**, 1236828 (2014).
76. S. E. Churchill, C. Vansickle, Pelvic morphology in *Homo erectus* and early *Homo*. *Anat. Rec. (Hoboken)* **300**, 964–977 (2017).
77. R. L. Holloway, D. C. Broadfield, M. S. Yuan, *The Human Fossil Record*, *Brain Endocasts-The Paleoneurological Evidence* (John Wiley and Sons, 2004).
78. L. T. Gruss, D. Schmitt. The evolution of the human pelvis: Changing adaptations to bipedalism, obstetrics and thermoregulation. *Philos. Trans. R. Soc. B* **370**, 20140063 (2015).

79. G. Suwa *et al.*, The *Ardipithecus ramidus* skull and its implications for hominid origins. *Science* **326**, 68–68e7 (2009).
80. T. D. White, C. O. Lovejoy, B. Asfaw, J. P. Carlson, G. Suwa, Neither chimpanzee nor human, *Ardipithecus* reveals the surprising ancestry of both. *Proc. Natl. Acad. Sci. U.S.A.* **112**, 4877–4884 (2015).
81. K. Sano *et al.*, A 1.4-million-year-old bone handaxe from Konso, Ethiopia, shows advanced tool technology in the early Acheulean. *Proc. Natl. Acad. Sci. U.S.A.* **117**, 18393–18400 (2020).
82. S. Semaw *et al.*, 2.5-million-year-old stone tools from Gona, Ethiopia. *Nature* **385**, 333–336 (1997).
83. S. P. McPherron *et al.*, Evidence for stone-tool-assisted consumption of animal tissues before 3.39 million years ago at Dikika, Ethiopia. *Nature* **466**, 857–860 (2010).
84. J. Yravedra, S. Rubio-Jara, L. A. Courtenay, J. A. Martos, Mammal butchery by *Homo erectus* at the Lower Pleistocene acheulean site of Juma's korongo 2 (JK2), bed III, Olduvai Gorge, Tanzania. *Quat. Sci. Rev.* **249**, 106612 (2020).
85. K. Isler, C. P. van Schaik, How our ancestors broke through the gray ceiling: Comparative evidence for cooperative breeding in early *Homo*. *Curr. Anthropol.* **53** (S6), S453–S465 (2012).
86. S. Shultz, E. Nelson, R. I. Dunbar, Hominin cognitive evolution: Identifying patterns and processes in the fossil and archaeological record. *Philos. Trans. R. Soc. Lond. B Biol. Sci.* **367**, 2130–2140 (2012).
87. A. Templeton, Out of Africa again and again. *Nature* **416**, 45–51 (2002).
88. A. Walker, C. Ruff, "The reconstruction of the pelvis" in *The Nariokotome Homo erectus Skeleton*, A. Walker, R. Leakey, Eds. (Harvard University Press, 1993).
89. C. Ruff, Body size and body shape in early hominins - implications of the Gona pelvis. *J. Hum. Evol.* **58**, 166–178 (2010).
90. S. W. Simpson *et al.*, A female *Homo erectus* pelvis from Gona, Ethiopia. *Science* **322**, 1089–1092 (2008).
91. S. W. Simpson, J. Quade, N. E. Levin, S. Semaw, The female *Homo* pelvis from Gona: Response to Ruff (2010). *J. Hum. Evol.* **68**, 32–35 (2014).
92. T. D. Weaver, J. J. Hublin, Neandertal birth canal shape and the evolution of human childbirth. *Proc. Natl. Acad. Sci. U.S.A.* **106**, 8151–8156 (2009).
93. C. B. Ruff, Biomechanics of the hip and birth in early *Homo*. *Am. J. Phys. Anthropol.* **98**, 527–574 (1995).
94. N. M. Laudicina, F. Rodriguez, J. M. DeSilva, Reconstructing birth in *Australopithecus sediba*. *PLoS One* **14**, e0221871 (2019).
95. M. F. Laird *et al.*, The skull of *Homo naledi*. *J. Hum. Evol.* **104**, 100–123 (2017).
96. T. W. Davies *et al.*, Distinct mandibular premolar crown morphology in *Homo naledi* and its implications for the evolution of *Homo* species in southern Africa. *Sci. Rep.* **10**, 13196 (2020).
97. R. L. Holloway *et al.*, Endocast morphology of *Homo naledi* from the Dinaledi Chamber, South Africa. *Proc. Natl. Acad. Sci. U.S.A.* **115**, 5738–5743 (2018).
98. J. D. Irish, M. Grabowski, Relative tooth size, Bayesian inference, and *Homo naledi*. *Am. J. Phys. Anthropol.* **176**, 262–282 (2021).
99. N. E. Levin, Environment and climate of early human evolution. *Annu. Rev. Earth Planet. Sci.* **43**, 405–429 (2015).
100. L. C. Aiello, C. Key, Energetic consequences of being a *Homo erectus* female. *Am. J. Hum. Biol.* **14**, 551–565 (2002).
101. W. R. Leonard, M. L. Robertson, On diet, energy metabolism, and brain size in human evolution. *Curr. Anthropol.* **37**, 125–129 (1996).
102. H. Pontzer, Ecological energetics in early *Homo*. *Curr. Anthropol.* **53** (S6), S346–S358 (2012).
103. R. I. Dunbar, Coevolution of neocortical size, group size and language in humans. *Behav. Brain Sci.* **16**, 681–694 (1993).
104. T. M. Grieco, O. T. Rizk, L. J. Hlusko, A modular framework characterizes micro- and macroevolution of Old World monkey dentitions. *Evolution* **67**, 241–259 (2013).
105. P. W. Lucas, R. T. Corlett, D. A. Luke, Postcanine tooth size and diet in anthropoid primates. *Z. Morphol. Anthropol.* **76**, 253–276 (1986).
106. S. Hillson, *Teeth* (Cambridge University Press, 2005).
107. R. Tacutu *et al.*, Human ageing genomic resources: Integrated databases and tools for the biology and genetics of ageing. *Nucleic Acids Res.* **41**, D1027–D1033 (2013).
108. L. E. Powell, K. Isler, R. A. Barton. Re-evaluating the link between brain size and behavioural ecology in primates. *Philos. Trans. R. Soc. B* **284**, 20171765 (2017).
109. R Core Team. R: A language and environment for statistical computing (R Foundation for Statistical Computing, Vienna, Austria, 2021).
110. RStudio Team, RStudio: Integrated development for R (RStudio, PBC, Boston, MA, 2021). https://www.rstudio.com/. Accessed 12 December 2021.
111. H. Wickham, *ggplot2: Elegant graphics for data analysis* (Springer, 2009), vol. 35.
112. H. Wickham, R. François, L. Henry, K. Müller, dplyr: A grammar of data manipulation (R Package Version 1.0.7., 2021). https://CRAN.R-project.org/package=dplyr. Accessed12 December 2021.
113. S. Faurby, J. C. Svenning, A species-level phylogeny of all extant and late Quaternary extinct mammals using a novel heuristic-hierarchical Bayesian approach. *Mol. Phylogenet. Evol.* **84**, 14–26 (2015).
114. E. Paradis, K. Schliep, ape 5.0: An environment for modern phylogenetics and evolutionary analyses in R. *Bioinformatics* **35**, 526–528 (2019).
115. D. Orme *et al.*, The caper package: Comparative analysis of phylogenetics and evolution in R (R package version, 5(2), 2013), pp. 1–36. https://cran.r-project.org/web/packages/caper/vignettes/caper.pdf. Accessed 12 December 2021.
116. Y. Haile-Selassie, S. M. Melillo, A. Vazzana, S. Benazzi, T. M. Ryan, A 3.8-million-year-old hominin cranium from Woranso-Mille, Ethiopia. *Nature* **573**, 214–219 (2019).
117. G. Suwa *et al.*, Paleobiological implications of the *Ardipithecus ramidus* dentition. *Science* **326**, 69–99 (2009).
118. T. Hogervorst, H. W. Bouma, J. de Vos, Evolution of the hip and pelvis. *Acta Orthop. Suppl.* **80**, 1–39 (2009).
119. C. Stringer, The origin and evolution of *Homo sapiens*. *Philos. Trans. R. Soc. B* **371**, 20150237 (2016).